Correlation Spectroscopy

When NMR spectroscopy is used to elucidate molecular structure, the assignment of the resonances is often the weakest link in the chain of evidence. Comparison with the spectra of similar molecules, and the organic chemist's knowledge of the trends in chemical shielding, usually provide the required information, but where these methods fail, recourse must be made to further NMR experiments such as double-resonance or cross-relaxation studies. Two-dimensional spectroscopy* (1) has now taken over from double-resonance methods, and a particularly useful form for assignment purposes is called *correlation spectroscopy*. (An earlier use of the same term to mean high-resolution spectroscopy examined by rapid-passage methods has now fallen into disuse.) Correlation is now taken to mean the identification of chemical sites that are related by a resolvable spin–spin coupling.

HETERONUCLEAR CORRELATION SPECTROSCOPY

Consider the simple case of correlation of proton and carbon-13 chemical shifts. We might employ polarization transfer* in the directions H $\rightarrow$ C or C $\rightarrow$ H, or we might exploit the inherently higher sensitivity of 'round-trip' transfer H $\rightarrow$ C $\rightarrow$ H. Since direct (single-bond) CH couplings are very much larger than long-range couplings, the experiment can be set up so that essentially all the polarization transfer occurs via the direct route (2). For simplicity, the H $\rightarrow$ C correlation technique is analysed here (3). Basically the experiment labels the proton frequencies by allowing free proton precession during the evolution period t_1 and identifies the directly coupled carbon-13 sites by detecting these resonances during the acquisition period t_2. The key is the transfer step when polarization is passed from each proton to a *specific* carbon site, just as runners in a relay race pass on the baton to a *designated* team-mate. A peak in the resulting two-dimensional spectrum has an F_1 frequency equal to the proton chemical shift and an F_2 frequency equal to the correlated carbon-13 chemical shift. Such a response is known as a *cross-peak* (4). This spectrum is conveniently displayed as an intensity contour map, since we are rather more interested in the frequencies than the relative intensities.

The observed carbon-13 signal is restricted to the transferred polarization; any 'natural' carbon-13 signal is suppressed by difference spectroscopy, since it serves no useful purpose in correlation experiments. The proton polarization is inherently

four times stronger than the natural carbon-13 polarization ($\gamma_H = 4\gamma_C$) and, because protons relax rather faster than carbon-13 nuclei, the cycle time for repeating the measurement can be quite short, further improving the sensitivity. For the case of $C \rightarrow H$ or $H \rightarrow C \rightarrow H$ correlation, the intense signal from protons attached to carbon-12 nuclei must be suppressed. Bilinear rotation decoupling* is useful in this regard (5).

The simplest way to visualize the mechanism of correlation spectroscopy is in terms of spin population effects, based on the fact that coupled proton and carbon spins share the same energy levels. Perturbation of proton populations necessarily affects the carbon-13 populations, and this can be detected by a final carbon-13 'read' pulse. In this sense the method is related to 'selective population transfer' experiments which apply a soft 180° pulse to one of the carbon-13 satellites of the proton spectrum.

A pulse sequence suitable for $H \rightarrow C$ correlation spectroscopy is set out in Fig. 1. An initial 90° pulse excites proton magnetization along the +Y axis, represented by two vectors α and β which precess during the first part of the evolution period at frequencies $2\pi(\delta_H + \frac{1}{2}J_{IS})$ and $2\pi(\delta_H - \frac{1}{2}J_{IS})$ rad s^{-1} respectively (Fig. 2(a)). At the mid-point of the evolution period, a 180° pulse applied to carbon-13 reverses the α and β labels of these vectors so that they now precess at $2\pi(\delta_H - \frac{1}{2}J_{IS})$ and $2\pi(\delta_H + \frac{1}{2}J_{IS})$ rad s^{-1} respectively (Fig. 2(b)). The net precession angle at the end of the evolution period is therefore $\theta = 2\pi\delta_H t_1$ radians; the spin–spin coupling term has been removed (Fig. 2(c)). As a result, CH splittings do not appear in the F_1 dimension of the correlation spectrum. The fixed interval $\Delta_1 = 1/(2J_{CH})$ allows these parallel vectors to diverge into the antiparallel orientation in preparation for the actual polarization transfer (Fig. 2(d)).

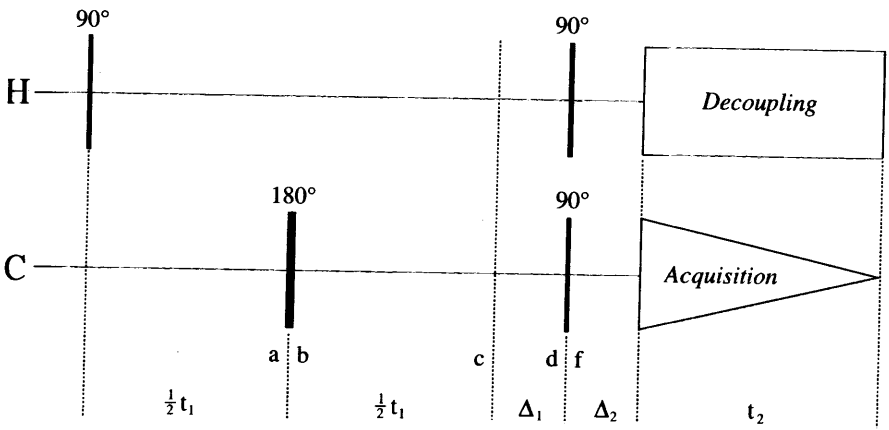

Fig. 1. Pulse sequence for heteronuclear correlation spectroscopy employing polarization transfer from protons to carbon-13. The timing markers a through f refer to the vector diagram of Fig. 2. The CH splittings are removed in both frequency dimensions.

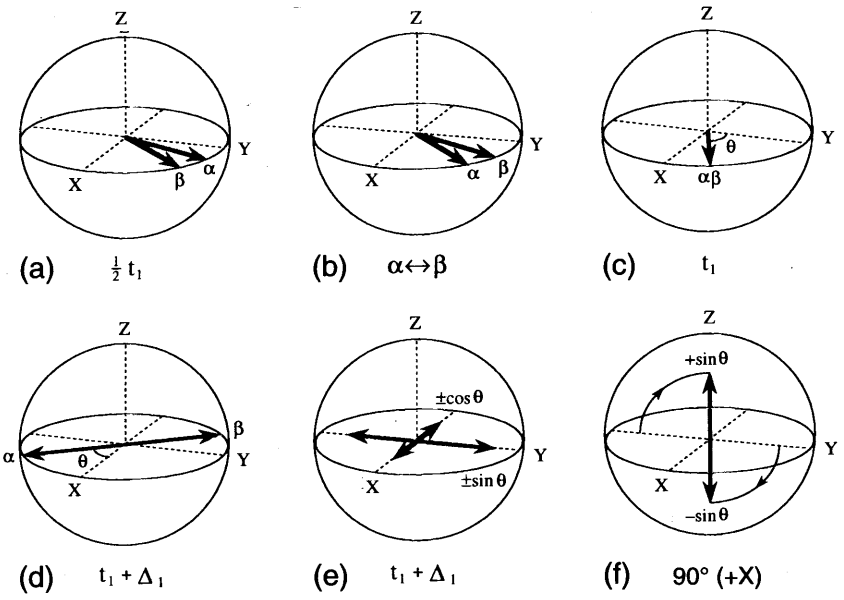

Fig. 2. Schematic diagram illustrating the motion of the proton vectors during a heteronuclear polarization transfer. (a) After a period $\frac{1}{2}t_1$ of free precession. (b) The effect of the 180° pulse on carbon-13. (c) Refocusing after a further period $\frac{1}{2}t_1$ of free precession. (d) Evolution into an antiphase configuration. (e) Vectors resolved into components along ±X and ±Y. (f) The Y components converted into longitudinal magnetization.

We now resolve these two vectors into their components ±M cos θ along the ±X axis, and ±M sin θ along the ±Y axis (Fig. 2(e)). The 90° pulse applied about the +X axis rotates the latter components into the ±Z axes (a population disturbance), but converts the former component into unobservable multiple-quantum coherence* which is never heard from again. These non-equilibrium spin populations are similar to those that would be created by a line-selective 180° pulse, but the amplitude of the disturbance is modulated by sin θ; this is how the proton chemical shift information is coded into the final two-dimensional spectrum. Because the carbon-13 spins share energy levels with the protons, the population disturbance also affects carbon-13 (Fig. 3(b)). If we express the *changes* in populations as a ratio of the equilibrium populations, they are +2a sin θ for one carbon-13 transition and −2a sin θ for the other, compared with the equilibrium population differences 2b, where the ratio $a/b = \gamma_H/\gamma_C = 4$. These population disturbances are converted into observable carbon-13 signals by the 90° 'read' pulse, giving an antiphase absorption-mode signal. Note that the last two 'simultaneous' 90° pulses can be taken in either order; it is convenient to consider the proton 90° pulse first, since then the mechanism can be described in terms of a disturbance of the spin populations. Had we made the other choice, we would have had to embark on a short excursion into multiple-quantum coherence.

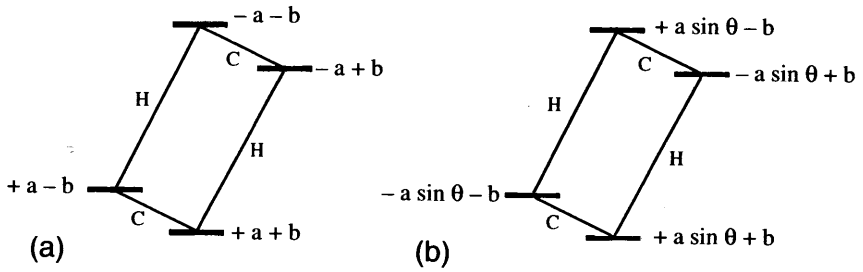

Fig. 3. Spin populations on the energy-level diagram for a proton (H) coupled to a carbon-13 spin (C). (a) At Boltzmann equilibrium the proton population differences are 2a, and the carbon-13 population differences are 2b, where a/b = 4. (b) After partial inversion of the proton populations, the carbon-13 population differences change by ±2a sin θ.

The second fixed delay Δ_2 allows the antiphase carbon-13 vectors to precess into alignment so that broadband proton decoupling can be imposed without fear of signal cancellation. For a CH group, Δ_2 is set equal to $1/(2J_{CH})$, but in general there may be CH_2 and CH_3 groups, and a compromise setting must be found, for example $\Delta_2 = 1/(3.3J_{CH})$. In this manner, the CH splitting has now been removed from *both* frequency dimensions, giving a particularly simple correlation spectrum. The only caveat is to beware of strong coupling effects between protons, remembering that this means between *carbon-13 satellites,* not between the main proton resonances.

HOMONUCLEAR CORRELATION SPECTROSCOPY

Proton–proton correlation spectroscopy was in fact the very first two-dimensional experiment (1) and it pioneered this new field of research. Homonuclear correlation spectroscopy, usually called COSY, exhibits some important differences with respect to the heteronuclear case treated above. There is no scope for 'decoupling' the active splitting J_{IS} because a 180° pulse would now affect both I and S. The coupling constants lie in a smaller, continuous range, and the rates of polarization transfer depend on the magnitudes of the active coupling constants. The contour map (6) is basically square in shape rather than rectangular; both axes span the same range of chemical shifts.

The COSY pulse sequence is deceptively simple:

$$90° - t_1 - 90° \text{ acquisition } (t_2). \qquad [1]$$

Normally the mechanism is described as coherence transfer, and is analysed by the density matrix or product operator formalisms (4), but it can be treated more simply in terms of population disturbances, just as in the heteronuclear case above.

We consider a weakly coupled two-spin (IS) system. Since the problem is symmetrical with respect to the I and S spins, we can concentrate simply on the $I \rightarrow S$ transfer which generates a cross-peak centred at (δ_I, δ_S). The corresponding

$S \rightarrow I$ transfer gives a symmetrically related cross-peak centred at (δ_S, δ_I).

The I-spin magnetization is represented by two equal vectors (M_0). After excitation by the first 90° pulse, they are initially aligned along the +Y axis and precess in the XY plane through angles

$$\theta_1 = (2\pi\delta_H + \pi J_{IS})t_1 \qquad [2]$$

$$\theta_2 = (2\pi\delta_H - \pi J_{IS})t_1. \qquad [3]$$

We resolve these vectors into $M_0 \sin\theta_1$ and $M_0 \sin\theta_2$ along the X axis, and $M_0 \cos\theta_1$ and $M_0 \cos\theta_2$ along the Y axis. The second 90° pulse is treated as a cascade of two 90° pulses, the first applied to the I spins and the second (a read pulse) applied to the S spins. The 90° pulse on the I spins rotates the Y components into the –Z axis but leaves the X components unchanged. Now a vector M_0 aligned along the –Z axis corresponds to a complete population inversion. We can represent this as a disturbance of the spin populations on a four-level diagram (Fig. 4). If $t_1 = 0$, $\cos\theta_1 = \cos\theta_2 = 1$, and there is complete population inversion across both I-spin transitions, but this leaves the population differences across the S-spin transitions unchanged. Only if the two I-spin transitions suffer *differential* population inversions ($\theta_1 \neq \theta_2$) does this affect the S-spin populations. The effect is of the same magnitude for the two S-spin transitions, but in opposite senses, giving the differential population disturbance:

$$\Delta p = \pm a(\cos\theta_2 - \cos\theta_1). \qquad [4]$$

Through a standard trigonometrical identity this can be rewritten as

$$\pm 2a \sin[\tfrac{1}{2}(\theta_1 + \theta_2)] \sin[\tfrac{1}{2}(\theta_1 - \theta_2)] = \pm 2a \sin(2\pi\delta_I t_1) \sin(\pi J_{IS} t_1). \qquad [5]$$

This tells us that the polarization transfer to the S spins builds up quite slowly, as a function of $\sin(\pi J_{IS} t_1)$, so if the maximum evolution time is too short, or if the I-spin signal decays too rapidly (broad lines compared with J_{IS}), then the transfer is negligible. The expression in eqn [5] also indicates that the cross-peak will be

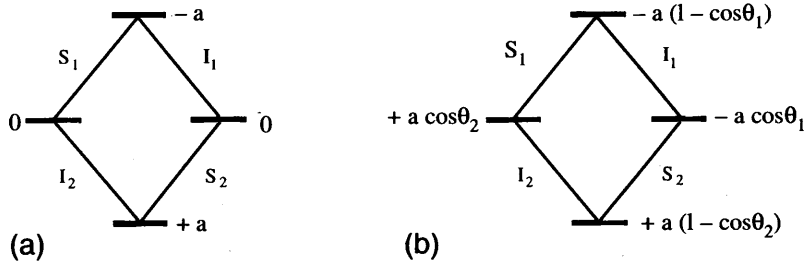

Fig. 4. Spin populations for a weakly coupled homonuclear two-spin (IS) system. (a) At Boltzmann equilibrium. (b) After partial spin inversions across the I-spin transitions. Only a differential disturbance ($\theta_1 \neq \theta_2$) affects the S-spin population differences.

centred at δ_I in the F_1 dimension and will have an antiphase doublet structure, the Fourier transform of the term $\sin(\pi J_{IS} t_1)$. The signal is detected at the S-spin frequency so the cross-peak is centred at δ_S in the F_2 dimension, and because the two S-spin transitions are affected in opposite senses, it will also have an antiphase doublet structure.

The characteristic shape of a COSY cross-peak is therefore an antiphase square pattern. Normally the spectrometer phase is adjusted so that cross-peaks appear in the absorption mode. We can draw the conclusion (mentioned above) that if the linewidth exceeds the splitting J_{IS}, there is mutual cancellation between positive and negative lines. In the limit the cross-peak vanishes.

It is convenient to designate I and S as 'active' spins, and the coupling J_{IS} as the 'active' coupling. When there are other spins coupled to I and S, they are called 'passive' spins and they introduce new splittings into the IS cross-peak. That is to say, a passive spin R converts δ_I and δ_S into effective chemical shifts, $(\delta_I \pm \frac{1}{2}J_{IR})$ and $(\delta_S \pm \frac{1}{2}J_{SR})$, each acting as a centre for the basic antiphase square patterns of lines. The cross-peak would therefore consist of 16 lines. We can easily pick out such patterns in the COSY spectrum of 2,3-dibromopropanoic acid (6) illustrated in Fig. 5(a).

This form of cross-peak is the most common but it only occurs when the second pulse of the COSY sequence is a 90° pulse. If a much smaller flip angle is chosen (45° is often used) the passive spins do not change their spin states during the experiment, but remain mere spectators. If the effective chemical shift in one dimension is $(\delta_I + \frac{1}{2}J_{IR})$ then the effective shift in the other dimension is $(\delta_S + \frac{1}{2}J_{SR})$, not $(\delta_S - \frac{1}{2}J_{SR})$. Instead of four basic square patterns, just two predominate, connected by a 'displacement vector' which is the resultant of J_{IR} and J_{SR}, taking account of their signs (Fig. 6). The sign of the slope of the displacement vector gives the relative signs of J_{IR} and J_{SR}. Thus a COSY spectrum with a 45° flip angle (Fig. 5(b)) shows examples of both like and opposite signs of the passive couplings.

So far we have neglected the components $M_0 \sin\theta_1$ and $M_0 \sin\theta_2$, which represent magnetization that remains at the I-spin site during the acquisition period. We might have expected that these two resonances would maintain their individual identities throughout t_1 and t_2 and thus give responses at the coordinates

$$\begin{aligned}&(\delta_I + \tfrac{1}{2}J_{IS},\ \delta_I + \tfrac{1}{2}J_{IS})\\&(\delta_I - \tfrac{1}{2}J_{IS},\ \delta_I - \tfrac{1}{2}J_{IS})\end{aligned} \qquad [6]$$

which lie exactly on the principal diagonal $F_1 = F_2$. This is to forget the influence of the second 90° pulse applied to the S spins. Had this been a 180° pulse, it would have interchanged the frequencies of the I-spin resonances, generating lines at the coordinates

$$\begin{aligned}&(\delta_I + \tfrac{1}{2}J_{IS},\ \delta_I - \tfrac{1}{2}J_{IS})\\&(\delta_I - \tfrac{1}{2}J_{IS},\ \delta_I + \tfrac{1}{2}J_{IS})\end{aligned} \qquad [7]$$

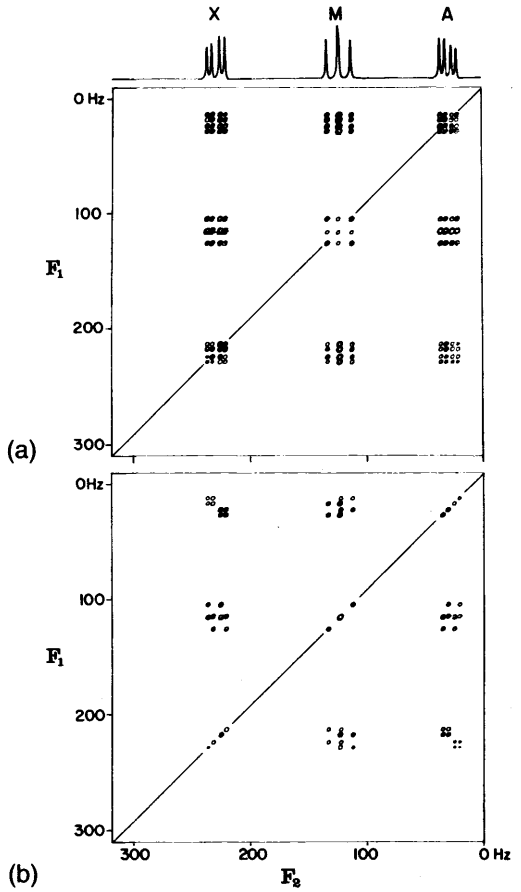

Fig. 5. COSY spectra of a three-spin system (a) with a 90° final pulse and (b) with a 45° final pulse. In spectrum (a) cross-peaks and diagonal peaks are 4 × 4 rectangular patterns. In spectrum (b) the cross-peaks consist of only two square patterns, and the slope of the displacement vector gives the relative signs of the two passive couplings; the diagonal peaks fall exactly on the diagonal (see text).

which lie just off the principal diagonal. On the other hand if the flip angle had been small, the S spins would have remained in the same state, and these lines would have fallen exactly on the principal diagonal (Fig. 5(b)). The actual 90° pulse has an intermediate effect, flipping the S spins in 50% of the cases, creating a square pattern of side J_{IS} straddling the diagonal. With the normal spectrometer phase setting, these diagonal peaks are in dispersion; there is no sign alternation.

Often we are interested in searching for weak cross-peaks close to the diagonal. Then it is a considerable advantage to employ double-quantum filtration in conjunction with the COSY experiment (7). The diagonal peaks (like the cross-peaks) are now principally in absorption and their tails are therefore less likely to

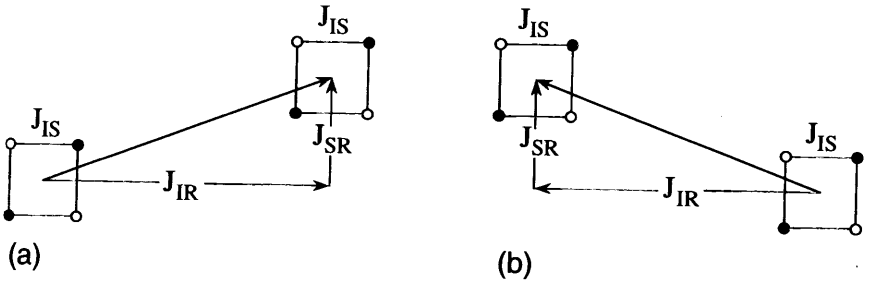

Fig. 6. Schematic diagram of a COSY cross-peak when the second pulse has a flip angle of 45° rather than 90°. (a) For like signs of the passive couplings J_{IR} and J_{SR}, giving a displacement vector with a positive slope. (b) For opposite signs, giving a displacement vector with a negative slope. Compare the experimental cross-peaks in Fig. 5(b).

obscure nearby cross-peaks. Furthermore, resonances from isolated spins, in particular intense solvent peaks, are suppressed since they cannot support double-quantum coherence.

REFERENCES

1. J. Jeener, Ampère International Summer School, Basko Polje, Yugoslavia, 1971, reported in *NMR and More. In Honour of Anatole Abragam,* ed. M. Goldman and M. Porneuf. Les Editions de Physique: Les Ulis, France, 1994.
2. A. A. Maudsley and R. R. Ernst, *Chem. Phys. Lett.* **50**, 368 (1977).
3. G. Bodenhausen and R. Freeman, *J. Magn. Reson.* **28**, 471 (1977).
4. W. P. Aue, E. Bartholdi and R. R. Ernst, *J. Chem. Phys.* **64**, 2229 (1976).
5. J. R. Garbow, D. P. Weitekamp and A. Pines, *Chem. Phys. Lett.* **93**, 514 (1982).
6. A. Bax and R. Freeman, *J. Magn. Reson.* **44**, 542 (1981).
7. U. Piantini, O. W. Sørensen and R. R. Ernst, *J. Am. Chem. Soc.* **104**, 6800 (1982).

Cross-references

Bilinear rotation decoupling
Coherence
Multiple-quantum coherence
Polarization transfer
Product operator formalism
Two-dimensional spectroscopy
Vector model